



RESEARCH ARTICLE

INTEGRATION OF TRIGONOMETRIC QUARTIC B-SPLINE COLLOCATION APPROACH
AND ADAMS-MOULTON SCHEME TO SOLVE THE EQUAL WIDTH EQUATION

Emre KIRLI¹, Mehmet Ali MERSİN^{2,*}

¹ Department, of Mathematics, Aksaray University, Aksaray, Türkiye
emre.26@windowslive.com - [0000-0002-5704-2370](https://orcid.org/0000-0002-5704-2370)

² Computer Programming, Aksaray University, Aksaray, Türkiye
mehmetalimersin@gmail.com - [000-0001-5125-8798](https://orcid.org/000-0001-5125-8798)

Abstract

This study focuses on the development of a novel numerical technique used to solve Equal Width (EW) equation. The spatial discretization of the EW equation is accomplished using a trigonometric quartic B-spline collocation technique. To achieve a fully discretized formulation of the EW equation, the third-order implicit Adams-Moulton method is employed. The efficiency and applicability of the recommended computational scheme are validated through numerical experiments, which include the analysis of single solitary wave propagation and the interaction of two solitary waves. The results obtained are compared with those from existing methods documented in the literature. These comparisons demonstrate that the proposed numerical scheme outperforms other methods in terms of accuracy.

Keywords

Quartic trigonometric B-spline,
Solitary wave,
Collocation method,
Adams-Moulton method

Time Scale of Article

Received :07 February 2025
Accepted : 16 May 2025
Online date : 25 June 2025

1. INTRODUCTION

Nonlinear dispersive wave equations play an important role in modeling many physical phenomena, such as the movement of shallow water waves. One of these equations is the Equal Width (EW) equation, introduced by Peregrine [1], which is considered a valuable replacement for the well-established Korteweg–de Vries (KdV) equation. The EW equation is written in the following form of

$$w_t + ww_x - \mu w_{xxt} = 0, \quad x \in [\alpha, \beta] \quad (1)$$

with the boundary conditions (BCs)

$$\begin{aligned} w(\alpha, t) = 0 & \quad w(\beta, t) = 0 \\ w_x(\alpha, t) = 0 & \quad w_x(\beta, t) = 0 \end{aligned}, \quad t \in (0, T) \quad (2)$$

and the initial condition (IC)

$$w(x, 0) = f(x), \quad x \in [\alpha, \beta] \quad (3)$$

where w describes the wave amplitude and the parameter μ is a positive constant.

*Corresponding Author: mehmetalimersin@gmail.com

Because of the nonlinear term in the EW equation, its exact solution can only be found under limited boundary and initial conditions. As a result, recent researches has mainly focused on computational methods, leading to the development of various numerical techniques for solving the EW equation. These techniques include the Petrov-Galerkin method [2, 3], lumped Galerkin method [4], B-spline Galerkin methods [5–9], B-spline collocation methods [10–14], the least-squares method [15], finite difference methods [16, 17], the RBF-PS scheme [18], meshless kernel-based methods [19], multiquadric quasi-interpolation [20], the Haar wavelet method [21], and a numerical method using polynomial scaling functions [22].

In this study, a novel numerical scheme is developed to derive approximate solutions for the EW equation. This scheme combines the trigonometric quartic B-spline collocation technique with the Adams-Moulton method. This work aims primarily to show how using the Adams-Moulton method for time integration affects the results. The paper is organized as follows: Section 2 discusses the time and space discretization of the EW equation. Section 3 examines the behavior and interaction of two solitary waves to test the impact and validity of the suggested method. The results are shown in tables, and a comparison is made between the proposed method and existing approaches. Finally, Section 4 provides an outline of the method's key discoveries and contributions of the method.

2. DISCRETIZATION SCHEME

To establish the temporal and spatial discretization of the EW equation, the domain $[\alpha, \beta] \times (0, T]$ is first discretized using uniformly distributed grid points (x_r, t_n) , where $x_r = \alpha + rh$, $r = 0, 1, \dots, M$ and $t_n = n\Delta t$, $n = 0, 1, \dots, N$. Here, h and Δt represent the spatial and temporal step sizes, respectively.

2.1. Temporal Discretization

Considering the EW equation of the form

$$v_t = (w - \mu w_{xx})_t = -ww_x \tag{4}$$

and utilizing the following one and two-step methods

$$v^{n+1} = v^n + \frac{\Delta t}{2}(v_t^{n+1} + v_t^n) + O(\Delta t^3) \tag{5}$$

$$v^{n+1} = v^n + \Delta t \left(\frac{5}{12}v_t^{n+1} + \frac{2}{3}v_t^n - \frac{1}{12}v_t^{n-1} \right) + O(\Delta t^4) \tag{6}$$

we set up the temporal integration of the Equation (4). The methods given in Equation (5) and Equation (6) can be rewritten in the general form as

$$v^{n+1} = v^n + \Delta t(\theta_1 v_t^{n+1} + \theta_2 v_t^n + \theta_3 v_t^{n-1}) \tag{7}$$

Selecting the coefficients in Equation (7) as $\theta_1 = \frac{1}{2}, \theta_2 = \frac{1}{2}, \theta_3 = 0$ provides Crank - Nicolson (CN) method which is second order in time and substituting the coefficients in Equation (7) as $\theta_1 = \frac{5}{12}, \theta_2 = \frac{2}{3}, \theta_3 = -\frac{1}{12}$ yields the two-step implicit Adams Moulton scheme. Using Equation (7), the temporal integration of the Equation (4) is achieved as

$$w^{n+1} - \mu w_{xx}^{n+1} + \theta_1 \Delta t w^{n+1} w_x^{n+1} = w^n - \mu w_{xx}^n - \theta_2 \Delta t w^n w_x^n - \theta_3 \Delta t w^{n-1} w_x^{n-1} \tag{8}$$

2.1. Spatial Discretization

Consider subdividing the spatial domain $[a, b]$ into M uniformly spaced finite elements at the specified points

$$\alpha = x_0 < x_1 < \dots < x_M = \beta \tag{9}$$

Then, the quartic trigonometric B-splines $T_r^4(x)$, $r = -2, \dots, M + 1$, at these knots are derived by the recurrence relation given in [23] as

$$T_r^4(x) = \frac{1}{\theta} \begin{cases} \rho^4(x_{r-2}), & x_{r-2} \leq x < x_{r-1}, \\ -\rho^3(x_{r-2})\rho(x_r) - \rho^2(x_{r-2})\rho(x_{r+1})\rho(x_{r-1}) \\ -\rho(x_{r-2})\rho(x_{r+2})\rho^2(x_{r-1}) - \rho(x_{r+3})\rho^3(x_{r-1}), & x_{r-1} \leq x < x_r, \\ \rho^2(x_{r-2})\rho^2(x_{r+1}) + \rho(x_{r-2})\rho(x_{r+2})\rho(x_{r-1})\rho(x_{r+1}) \\ +\rho(x_{r-2})\rho^2(x_{r+2})\rho(x_r) + \rho(x_{r+3})\rho^2(x_{r-1})\rho(x_{r+1}) \\ +\rho(x_{r+3})\rho(x_{r-1})\rho(x_{r+2})\rho(x_r) + \rho^2(x_{r+3})\rho^2(x_r), & x_r \leq x < x_{r+1}, \\ -\rho(x_{r-2})\rho^3(x_{r+2}) - \rho(x_{r+3})\rho(x_{r-1})\rho^2(x_{r+2}) \\ -\rho^2(x_{r+3})\rho(x_r)\rho(x_{r+2}) - \rho^3(x_{r+3})\rho(x_{r+1}), & x_{r+1} \leq x < x_{r+2}, \\ \rho^4(x_{r+3}), & x_{r+2} \leq x < x_{r+3}, \\ 0, & otherwise \end{cases} \tag{10}$$

where

$$\theta = \sin\left(\frac{h}{2}\right) \sin(h) \sin\left(\frac{3h}{2}\right) \sin(2h)$$

$$\rho(x_r) = \sin\left(\frac{x - x_r}{2}\right)$$

The collection of the quartic trigonometric B-spline functions $\{T_{-2}^4(x), T_{-1}^4(x), \dots, T_M^4(x), T_{M+1}^4(x)\}$ creates a basis for the smooth functions defined across the spatial domain.

To perform the spatial integration of Equation (1), we begin by assuming that $W(x, t)$ is the quartic trigonometric B-spline approximation to the exact solution $w(x, t)$ to the problem. Following that form $W(x, t)$ in terms of the trigonometric B-splines T_j^4 and the temporal terms $\delta_j(t)$ as

$$W(x, t) = \sum_{j=-2}^{M+1} \delta_j T_j^4 \tag{11}$$

where the temporal terms $\delta_j(t)$ will be calculated using the BCs and collocation method. Since each subinterval $[x_{r-1}, x_r]$ is represented by five quartic trigonometric B-spline functions, the unknown function W and its first two spatial derivatives at the knots x_r are calculated in terms of the temporal terms as

$$\begin{aligned} W_r &= a_1 \delta_{r-2} + a_2 \delta_{r-1} + a_2 \delta_r + a_1 \delta_{r+1} \\ W_r' &= b_1 \delta_{r-2} + b_2 \delta_{r-1} - b_2 \delta_r - b_1 \delta_{r+1} \\ W_r'' &= c_1 \delta_{r-2} - c_1 \delta_{r-1} - c_1 \delta_r + c_1 \delta_{r+1} \end{aligned} \tag{12}$$

where

$$\begin{aligned} a_1 &= \frac{\sin^4\left(\frac{h}{2}\right)}{\theta}, & a_2 &= \frac{\sin^4\left(\frac{h}{2}\right)\left(12\cos^2\left(\frac{h}{2}\right) - 1\right)}{\theta}, \\ b_1 &= -\frac{2\sin^3\left(\frac{h}{2}\right)\cos\left(\frac{h}{2}\right)}{\theta}, & b_2 &= -\frac{2\sin^3\left(\frac{h}{2}\right)\cos\left(\frac{h}{2}\right)\left(4\cos^2\left(\frac{h}{2}\right) - 1\right)}{\theta}, \\ c_1 &= \frac{\sin^2\left(\frac{h}{2}\right)\left(4\cos^2\left(\frac{h}{2}\right) - 1\right)}{\theta}. \end{aligned}$$

Using (12) in (8), the fully-discretized form of EW equation is obtained as

$$\begin{aligned} &\delta_{r-2}^{n+1}(\alpha_1 - \mu c_1 + \Delta t W_r^{n+1} b_1) + \delta_{r-1}^{n+1}(\alpha_2 + \mu c_1 + \theta_1 \Delta t W_r^{n+1} b_2) \\ &+ \delta_r^{n+1}(\alpha_2 + \mu c_1 - \theta_1 \Delta t W_r^{n+1} b_2) + \delta_{r+1}^{n+1}(\alpha_1 - \mu c_1 - \theta_1 \Delta t W_r^{n+1} b_1) \quad (13) \\ &= W_r^n - \mu(W_{xx})_r^n - \theta_2 \Delta t W_r^n (W_x)_r^n - \theta_3 \Delta t W_r^{n-1} (W_x)_r^{n-1}, \quad 0 \leq r \leq M. \end{aligned}$$

Hence, we achieve a system (13) involving $M + 1$ equations and $M + 4$ unknowns. Using the BCs (3) enables to equalize the number of equations and unknowns and the variables

$$\delta_{-2}^{n+1}, \delta_{-1}^{n+1} \text{ and } \delta_{M+1}^{n+1}$$

are eliminated from the system (13), simplifying it into a solvable $(M + 1) \times (M + 1)$ matrix system. So as to commence the iterative procedure, the initial vectors $\delta^0 = (\delta_{-2}^0, \delta_{-1}^0, \dots, \delta_{M+1}^0)^T$ and $\delta^1 = (\delta_{-2}^1, \delta_{-1}^1, \dots, \delta_{M+1}^1)^T$ need to be computed. The initial vector δ^0 is first calculated by the use of IC and BCs as follows :

$$\begin{aligned} W'(\alpha, 0) &= 0 \\ W''(\alpha, 0) &= 0 \\ W(x_r, 0) &= f(x_r) \\ W'(\beta, 0) &= 0 \end{aligned}$$

where $r = 0, 1, \dots, M$. Then, the other initial vector δ^1 is achieved by using CN technique. Therefore, the unknown vector $\delta^{n+1} = (\delta_{-2}^{n+1}, \delta_{-1}^{n+1}, \dots, \delta_{M+1}^{n+1})^T$ ($n = 1, 2, \dots$) can be computed iteratively at any desired time by using two previous δ^n and δ^{n-1} unknown vectors. Since we have an implicit system (13) with respect to the term δ , an inner iterative algorithm is used three times at all-time steps to obtain better accuracy.

3. NUMERICAL RESULTS

This section presents two test problems to demonstrate the efficiency and applicability of the proposed scheme. The accuracy of the solution is assessed by calculating the error norm L_∞

$$L_\infty = \max_m |w_m - W_m|, \quad (14)$$

and the following formulae is used to calculate the order of the temporal-convergence

$$order = \frac{\log \left| \frac{(L_\infty)_{\Delta t_i}}{(L_\infty)_{\Delta t_{i+1}}} \right|}{\log \left| \frac{\Delta t_i}{\Delta t_{i+1}} \right|} \quad (15)$$

where $(L_\infty)_{\Delta t_i}$ represents the error norm L_∞ for temporal step Δt_i . The three invariants corresponding to mass I_1 , momentum I_2 and energy I_3 are worked out by means of the following formulae [24]

$$I_1 = \int_{-\infty}^{\infty} w dx \approx \int_{\alpha}^{\beta} W dx$$

$$I_2 = \int_{-\infty}^{\infty} (w^2 + \mu(w_x)^2) dx \approx \int_{\alpha}^{\beta} (W^2 + \mu(W_x)^2) dx$$

$$I_3 = \int_{-\infty}^{\infty} w^3 dx \approx \int_{\alpha}^{\beta} W^3 dx$$

The trapezoidal rule for the spatial domain $[\alpha, \beta]$ is employed to evaluate approximately the above integrals at all-time steps.

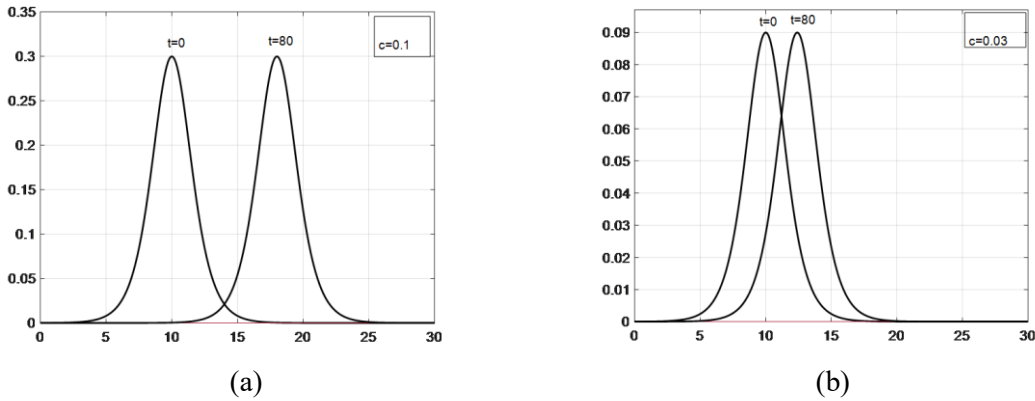


Figure 1. $W(x, t)$ for $h = 0.1$ and $\Delta t = 0.1$

3.1. Motion of a Single Solitary Wave

In the first test problem, the analytical single solitary wave solution of the EW equation is expressed with equation:

$$w(x, t) = 3c \operatorname{sech}^2(k[x - \tilde{x}_0 - vt]) \quad (16)$$

in which the velocity of the solitary wave $v = c$, amplitude of the solitary wave is $3c$, $k = \sqrt{\frac{c}{4\mu v}}$ represents the width of the solitary wave and \tilde{x}_0 denotes the initial wave peak position. The BCs are set to zero at both ends. By taking $t = 0$ in the analytical solution (16), the IC is obtained as

$$w(x, 0) = 3c \operatorname{sech}^2(k[x - \tilde{x}_0]) \quad (17)$$

Using IC (16) in the integrals I_1, I_2, I_3 , the analytical values of three invariants are calculated for the first problem as follows

$$I_1 = \frac{6c}{k}, I_2 = \frac{12c^2}{k} + \frac{48k\mu c^2}{5}, I_3 = \frac{144c^3}{5k}$$

The calculations are done with the parameters $\mu = 1, \tilde{x}_0 = 10$, amplitudes $3c = 0.3, 3c = 0.09$. The graphs of the simulations of the single solitary wave for various values of c at $t = 0$ and $t = 80$ are displayed in Figure 1. It is obvious from Figure 1 that the solitary wave maintains its initial shape, velocity and amplitude during the simulation. The algorithm is run up to $t = 80$ over various spatial domains with different temporal and spatial step widths. The error norm L_∞ and three invariants are reported in Table 1a and Table 1b to compare the present method with existing methods. The comparison demonstrates that the proposed method yields significantly more accurate results than the existing techniques outlined in [2, 3, 4, 5, 6, 14, 21]. Additionally, the invariants computed using the present method align closely with the analytical values, as illustrated in Table 1a and Table 1b. Table 2a and Table 2b present the conservation invariants, temporal rate of convergence, and error norms, which confirm that for a fixed spatial step size, reducing the temporal step size from 2 to 0.25 results in a numerical convergence rate approaching three. Furthermore, the computed invariants remain consistent with their analytical counterparts. Figure 2 displays the absolute error plot for the parameters $c = 0.1, h = 0.05$, and $\Delta t = 0.25$.

Table 1a. Error norms and invariants of single solitary wave for $c = 0.1, h = 0.03, \Delta t = 0.05, 0 \leq x \leq 30$ at $t=80$

Method	I_1	I_2	I_3	L_∞
Present Method	1.19999	0.28800	0.05760	7.37×10^{-6}
[2]	1.19100	0.28550	0.05582	2.64×10^{-3}
[5]	1.23387	0.29915	0.06097	1.64×10^{-2}
[4]	1.19995	0.28798	0.05759	2.10×10^{-5}
[3]	1.20004	0.28880	0.05760	5.15×10^{-5}
[14]	1.19999	0.28800	0.05760	9.60×10^{-6}
[21]	1.19999	0.28799	0.05759	1.26×10^{-5}
Analytical	1.2	0.288	0.0576	–

Table 1b. Error norms and invariants of single solitary wave for $c = 0.03, h = 0.1, \Delta t = 0.1, 0 \leq x \leq 30$ at $t=80$

Method	I_1	I_2	I_3	L_∞
Present Method	0.3599970	0.0259200	0.0015552	1.48×10^{-6}
[6] QBGM	0.3599964	0.0259252	0.0015525	2.09×10^{-6}
Analytical	0.36	0.02592	0.00155520	–

Table 2a. Error norms, invariants and order of convergence with $c = 0.1, h = 0.05, -10 \leq x \leq 40$ at $t=80$

Δt	I_1	I_2	I_3	L_∞	order
2	1.199050	0.288127	0.057365	2.96×10^{-4}	–
1	1.199882	0.288016	0.057605	3.64×10^{-5}	3.02
0.5	1.199998	0.288002	0.576001	4.50×10^{-6}	3.02
0.25	1.199999	0.288000	0.576001	5.47×10^{-7}	3.04

Table 2b. Error norms, invariants and order of convergence with $c = 0.03, h = 0.05, -10 \leq x \leq 40$ at $t=80$

Δt	I_1	I_2	I_3	L_∞	order
2	0.359998	0.025920	0.001555	1.24×10^{-6}	–
1	0.360000	0.025920	0.001555	1.54×10^{-7}	3.00
0.5	0.360000	0.025920	0.001555	1.89×10^{-8}	3.03
0.25	0.360000	0.025920	0.001555	2.53×10^{-9}	2.90

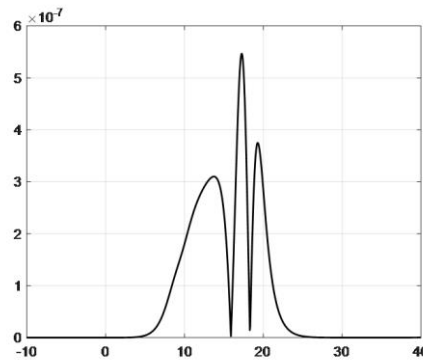


Figure 2. Absolute error at $t = 80$

3.1. Interaction of Two Solitary Waves

In the problem of interaction of two solitary waves, the following IC is tackled

$$w(x, 0) = 3c_1 \operatorname{sech}^2\left(\frac{1}{2}[x - \tilde{x}_1 - c_1]\right) + 3c_2 \operatorname{sech}^2\left(\frac{1}{2}[x - \tilde{x}_2 - c_2]\right) \quad (18)$$

where the parameters $\mu = 1, c_1 = 1.5, c_2 = 0.75, \tilde{x}_1 = 10$ and $\tilde{x}_2 = 25$ are selected.

These parameters yield two well-separated solitary waves initially situated at \tilde{x}_1 and \tilde{x}_2 and moving in the same directions. To make a comparison our results with the results of the method given in [18], the algorithm is run on the spatial domain $[0, 80]$ with time step $\Delta t = 0.05$ and space step $h = 0.2$ until $t = 30$. Simulation of the interaction process is given in Figure 3. As shown in Figure 3, the interaction takes place at nearly $t = 15$ and then two waves proceed without change their original shape. The values of analytical invariants are determined as

$$\begin{aligned} I_1 &= 12(c_1 + c_2) = 27, \\ I_2 &= 28.8(c_1^2 + c_2^2) = 81, \\ I_3 &= 57.6(c_1^3 + c_2^3) = 218.7. \end{aligned}$$

The comparison of the computed invariants with invariants presented by the method [18] is given in Table 3. It can obviously be seen that the three invariants computed by the present method are closer to the analytical values of the invariants. Also, the calculated invariants are reported in Table 4 at various time levels. When Table 4 is examined, the calculated invariants are observed to align with the analytical values throughout the interaction process

Table 3. Comparison of the invariants for the interaction of two solitary waves at $t = 30$

	Present Method	[18](RK4)
I_1	26.99643	26.92975
I_2	81.00892	80.79845
I_3	218.73882	218.15719

Table 4. Invariants for the interaction of two solitary waves with $h = 0.2, \Delta t = 0.05$ at various time levels

t	I_1	I_2	I_3
1	26.99948	81.00053	218.70239
5	26.99928	81.00173	218.70778
10	26.99858	81.00322	218.71455
15	26.99810	81.00457	218.71992
20	26.99778	81.00560	218.72461
25	26.99714	81.00739	218.73210
30	26.99643	81.00892	218.73882
Exact	27	81	218.7

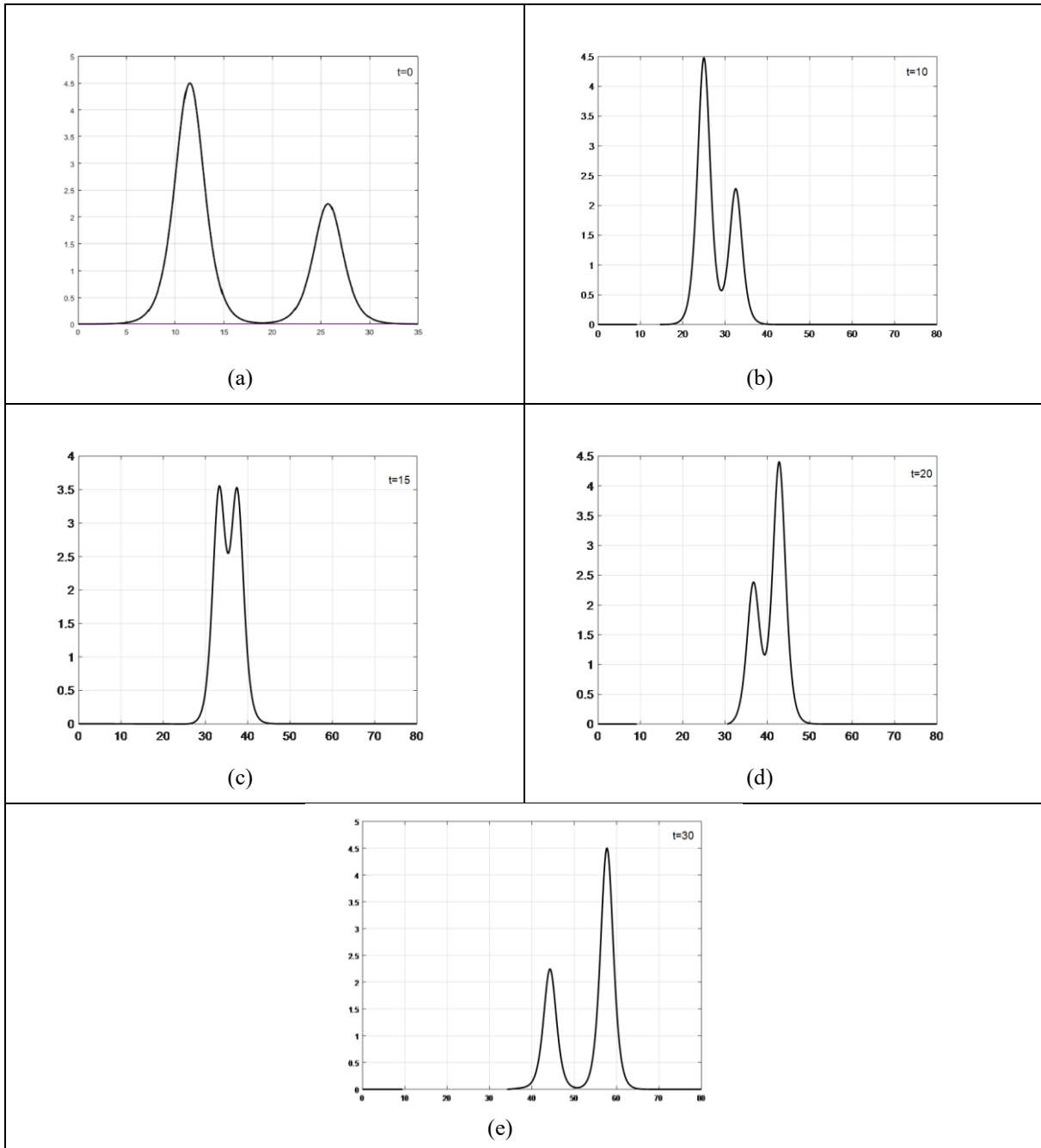


Figure 3. The simulation of interaction process

4. CONCLUSION

In the present work, a novel numerical scheme is introduced to derive approximate solutions for the EW equation. This scheme is developed by integrating the trigonometric quartic B-spline collocation technique with the third-order implicit Adams-Moulton method. To evaluate the performance and efficiency of the proposed approach, two test problems are investigated, focusing on the behavior of a solitary wave and the interaction between two solitary waves. The results demonstrate that the error norms produced by the present method are significantly smaller than studies of [2, 3, 4, 5, 6, 14, 21]. The invariant constants are computed numerically and compared with their analytical values, revealing that the invariants remain well-preserved throughout the simulation. This indicates an accurate representation of soliton propagation and interaction. Additionally, the calculated temporal rate of convergence aligns closely with the theoretical value. In conclusion, the proposed numerical scheme offers notable advantages in terms of both accuracy and computational efficiency, making it a highly suitable method for addressing problems that model physical phenomena in engineering and scientific applications.

ACKNOWLEDGEMENTS

Acknowledgments of people, grants, funds, etc. should be placed in a separate section before the reference list. The names of funding organizations should be written in full.

CONFLICT OF INTEREST

The authors stated that there are no conflicts of interest regarding the publication of this article.

CRedit AUTHOR STATEMENT

Emre Kırlı: Methodology, Supervision, Software, Conceptualization, **Mehmet Ali Mersin:** Writing-Original Draft, Visualization, Writing-Review & Editing, Supervision

REFERENCES

- [1] Morrison PJ, Meiss JD, Carey JR. Scattering of RLW solitary waves. *Physica D* 1984; 11(3): 324-336.
- [2] Gardner LRT, Gardner GA, Ayoub FA, Amein NK. Simulations of the EW undular bore. *Commun Numer Methods Eng* 1997; 13(7): 583-592.
- [3] Roshan T. A Petrov-Galerkin method for equal width equation. *Appl Math Comput* 2011; 218(6): 2730-2739.
- [4] Esen A. A numerical solution of the equal width wave equation by a lumped Galerkin method. *Appl Math Comput* 2005; 168(1): 270-282.

- [5] Doğan A. Application of Galerkin's method to equal width wave equation. *Appl Math Comput* 2005; 160(1): 65-76.
- [6] Irk D. B-Spline Galerkin solutions for the equal width equation. *Phys Wave Phenom* 2012; 20(2): 122-130.
- [7] Saka B. A finite element method for equal width equation. *Appl Math Comput* 2006; 175(1): 730-747.
- [8] Saka B, Dağ I, Dereli Y, Korkmaz A. Three different methods for numerical solution of the EW equation. *Eng Anal Bound Elem* 2008; 32(7): 556-566.
- [9] Dağ I, Irk D, Boz A. Simulation of EW wave generation via quadratic B-spline finite element method. *Int J Math Stat* 2007; 1(A07): 46-59.
- [10] Zorşahin Görgülü M. A new algorithm based on the dedic (tenth degree) B-spline functions for numerical solution of the equal width equation. *J Eng Technol Appl Sci* (In press): DOI: 10.30931/jetas.1072151.
- [11] Raslan KR. Collocation method using quartic B-spline for the equal width (EW) equation. *Appl Math Comput* 2005; 168(2): 795-805.
- [12] Dağ I, Saka B. A cubic B-spline collocation method for the EW equation. *Math Comput Appl* 2004; 9(3): 381-392.
- [13] Dağ I, Ersoy Ö. The exponential cubic B-spline algorithm for equal width equation. *Adv Stud Contemp Math* 2015; 25(4): 525-535.
- [14] Yağmurlu NM, Karakaş AS. Numerical solutions of the equal width equation by trigonometric cubic B-spline collocation method based on Rubin-Graves type linearization. *Numer Methods Partial Differ Equ* 2020; 36(5): 1170-1183.
- [15] Zaki SI. A least-squares finite element scheme for the EW equation. *Commun Numer Methods Eng* 2000; 16(3): 177-190.
- [16] Banaja MA, Bakodah HO. Runge-Kutta integration of the equal width wave equation using the method of lines. *Math Probl Eng* 2015; 2015: Article ID 274579.
- [17] İnan B, Bahadır AR. A numerical solution of the equal width wave equation using a fully implicit finite difference method. *Turk J Math Comput Sci* 2014; 2(1): 1-14.
- [18] Uddin M. RBF-PS scheme for solving the equal width equation. *Appl Math Comput* 2013; 222: 619-631.
- [19] Dereli Y, Schaback R. The meshless kernel-based method of lines for solving the equal width equation. *Appl Math Comput* 2013; 219(10): 5224-5232.

- [20] Dhawan S, Ak T, Apaydın G. Algorithms for numerical solution of the equal width wave equation using multi-quadric quasi-interpolation method. *Int J Mod Phys C* 2019; 30(11): 1950087.
- [21] Ghafoor A, Haq S. An efficient numerical scheme for the study of equal width equation. *Results Phys* 2018; 9: 1411-1416.
- [22] Oruç Ö, Esen A, Bulut F. Highly accurate numerical scheme based on polynomial scaling functions for equal width equation. *Wave Motion* 2021; 105: 102760.
- [23] Lyche T, Winther R. A stable recurrence relation for trigonometric B-splines. *J Approx Theory* 1979; 25(3): 266-279.
- [24] Olver PJ. Euler operators and conservation laws of the BBM equation. *Math Proc Camb Philos Soc* 1979; 85(1): 143-159.